COBEM 2021 26th International Congress of Mechanical Engineering
November 22-26, 2021, Virtual Congress, Brazil

COB-2021-0269
Thermal Radiation Shielding Applied to Polymeric Repair

Robson Felipe Viana da Silva
Fabio Toshio Kanizawa
Universidade Federal Fluminense, Departamento de Engenharia Mecânica.
robsonfelipe@id.uff.br; fabiokanizawa@id.uff.br.

Abstract. *This study aims to experimentally investigate thermal radiation shielding systems focused on applications for polymeric matrix repairs of flare towers. The use of this type of repair in flare tower structure has restrictions due to the radiation emitted by the flame, which heats the repair above the material limiting operational temperature. The specimen evaluated consists of a cylindrical segment similar to the structural component of the flare towers. The specimen is positioned inside a chamber with a uniform and upward air flow at controlled low velocity to simulate the condition of natural convection. The chamber's walls inner surface are covered with a paint of high absorptivity to mitigate eventual effects of radiation reflection, and the temperature is controlled by a serpentine circuit fixed on its outer surface, to reduce eventual superheating and contribution on the radiation on the specimen. Thermal shields made with steel sheets and paintings will be analyzed. It is intended to evaluate specimens with diameters of 0.15 and 0.2 m (6 and 8 inches), with heat flux between 5 and 10 kW/m² at specimen. The main objective of the experiment is evaluating distinct geometrical configuration of the shielding for wide range of heat flux values. Additionally, it is expected to evaluate the temperature reduction of the repair due to the use of the shielding for distinct inclinations in relation to the heat source.*

Keywords: *radiation, shielding, flare, polymeric, repair.*

1. Introduction

A flare tower is an equipment present in the oil and natural gas extraction and refining plants. This tower is responsible for relieving the pressure of other equipment, controlling excessive production and disposing of material in case of an emergency. When the structure of a tower is damaged, using a repair made of polymeric matrix material is an interesting alternative to substation, which would be very costly and correspond to longer period of maintenance. Nonetheless, the performance and lifetime of these repairs are impacted by the presence of a constant heat flux from the flame at one end of the tower, which heats the polymer to temperatures above its operational limit, of approximately 200 °C.

Part of the thermal radiation emitted by the flames is absorbed by the structures in the vicinity, including the eventual repair, and results in increment of the temperature. The heating of the repair also occurs, on a smaller scale, from heat conduction and radiation among the structure elements, since it absorbs and reflects energy. The influence of the wind on the flame takes place in changing its shape and intensity, and for high speed winds, flare performance is impaired.

Cavalcanti (2011) presents a study on the influence of reflective surfaces as thermal insulators in order to reduce heat transfer. His experiment used three 430 stainless steel sheets, lined up in front of a heat source, with air, vacuum and glass wool coatings between them. The results show that the use of plates with glass wool coating showed greater efficiency in blocking radiation, as well as achieving stability at temperatures more quickly.

Viskanta (1965) proposes the use of an absorbent and dispersive gas layer for thermal shielding of surfaces. The analysis was performed based on the measurement of heat flux in a system composed of two plates with gas between them. It is observed that the thickness of the gas layer directly interferes with the blocking of radiation and that this application covers all incidence conditions.

Pereira (2016) uses a ceramic composite to optimize thermal radiation. The methodology is based on the characteristics of refractory materials to increase the rate of heat transfer by radiation. The result of the experiment presented shows that a specimen coated with this material has a lower temperature than the one that did not receive the coating.

Muratova (2017) features thermal shielding made of porous nanoparticle membrane based on anodic alumina. The properties of this membrane block infrared radiation in the range of 8 to 14 μm. In his results, Muratova presents a reduction of about 30 ºC when comparing the thermographic measurement of a surface.

The study developed by Kim *et al*. (2014) compares the use of shielding made by one-piece and perforated flat metal plates around a flare torch, showing a reduction in heat flux from 10 kW/m² to values close to zero at a distance of 1.5 m from the heat source for both cases. Furthermore, it reveals that the temperature tends to the ambient temperature at about 0.3 m away from the source.

This study aims to experimentally investigate the performance of thermal radiation shielding for polymeric repair in cylindrical structures, in order of limiting the temperature within the range of the material.

2. Experimental Facility

The experimental facility developed consists of a test chamber, a thermal radiation source, a water cooling system and a compressed air system. The scheme of the experimental set is seen in Figure 1. The test chamber is used for safety reasons due to the high heat fluxes, in addition to reducing the interference of the environment with the experiment. The refrigeration system works through a circuit of coils fixed to the external surface of the chamber, connected to an evaporative cooling tower. The compressed air system is used to generate a uniform upward stream of air inside the chamber, controlled at low values to mimic conditions of natural convection, without excessive heating of the air in the vicinity of the specimen, which would affect the measurement.

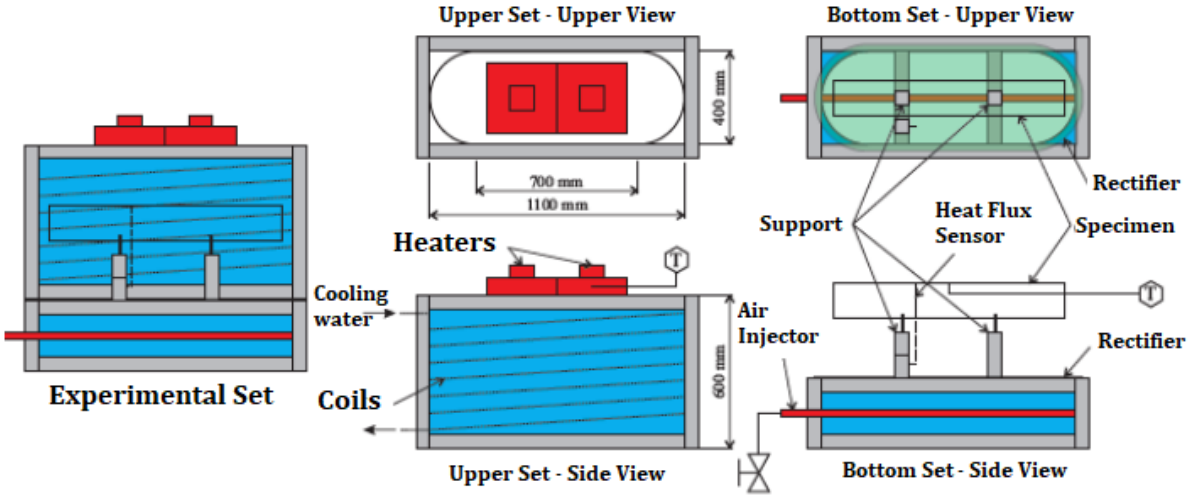

Figure 1. Scheme of the experimental set.

The radiation source plays the role of the flame present in the flare tower. The infrared heaters will be positioned at the top of the facility and centered on the horizontal plane, facing downwards. The face area of each heater is 0.3 x 0.3 m². The intensity of radiation emitted by a flare tower, according to Schwartz and White (1996), depends on factors such as the composition of the flare gas, the type of flare installation, the state of the gas-air mixture, the flame temperature and others. According to Kim *et al.* (2014), the actual heat flux emitted in a plant/platform is in the order of 400 kW/m². HSE (2006) presents the impacts on human life from heat flux values. Thus, the range of variation of the thermal radiation flux applied in the experiment was defined, with values from 5 to 10 kW/m².

Given the position of the source in the experimental facility, part of its radiation focuses on the test chamber and the other part focuses on the specimen. Due to the surface properties of the chamber, this energy will be partially absorbed and reflected. The reflection of radiation on the specimen generates an overheating with no existing correlation to the real scenario which the experiment is based on. Therefore, a paint with high absorptivity was used to cover the chamber's inner surface to reduce the reflectivity effect. Based on Dornelles *et al*. (2014) study, which investigates paint's absorptivity under solar radiation, a conventional black paint was selected to cover the chamber's inner surface, as it has the highest absorptivity in the infrared spectrum.

Since the radiation of a body is associated with the fourth power of its temperature, a cooling system for the test chamber was planned, expecting to reduce its radiation over the specimen. This cooling is done through water flow in a circuit of coils fixed to the chamber's external surface. These circuits are connected to an evaporative cooling tower. Figure 2 shows the complete scheme of the refrigeration system implemented in the experiments.

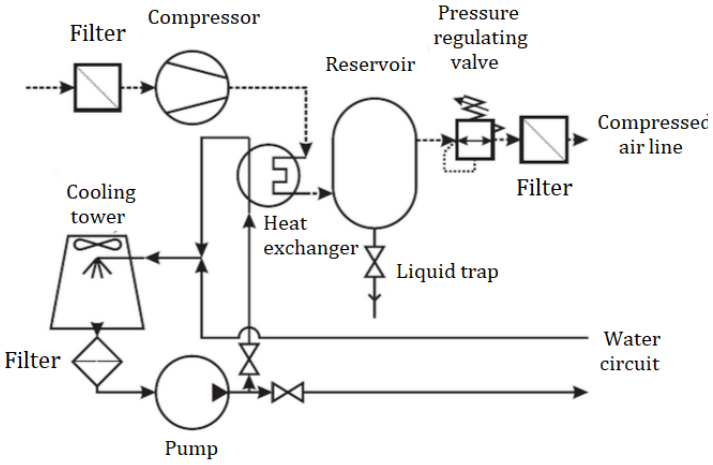

Figure 2. Cooling System Schematic.

It was necessary to stipulate the intensity of the heat flow radiated to the test chamber to design the cooling circuit. Equation (1) represents the generic formulation for calculating the form factor between these surfaces, demonstrated by Ozturk (2019), where A is the area, S is the distance between the surfaces, θ is the angle formed by the line connecting the surfaces with respect to their normal vectors v_n and the i and j indexes indicate to which surface these quantities belong. The distance between the specimen and the energy source is variable, impacting the "visibility" of the source in relation to the chamber. Therefore, the analysis was carried out considering the case of greater exposure from the chamber to the source. From the discretization of Equation (1), combined with a numerical method of finite differences, the form factor of the source for the internal surface of the test chamber was found, equivalent to 0.76, and thus the heat flux over the chamber was determined.

$$F_{Ai-Aj} = (1/A_i) \left(\int_{Ai} \int_{Aj} cos\theta_i cos\theta_j \, / (\pi \, S^2) \; dA_j dA_i \right). \tag{1}$$

For the analysis of the forced flow inside the coils, assumptions were made of constant heat flux, incompressible fluid, uniform flow velocity along the cross section equivalent to 1 m/s and temperature boundary conditions at the inlet and outlet of 29 °C and 34 °C, respectively. All water properties were defined at a temperature of 25ºC, considering the generated error.

The heat transferred in the system will be equivalent to the sum of the heat removed by each coil, as shown in Equation (2), where Q_C is the heat radiated to the chamber, n is the number of circuits and Q_S is the heat transferred by each coil. The rate of heat absorbed by the fluid is given by Equation (3), derived from the First Law of Thermodynamics, where m_a is the water mass flow, c is the water specific heat, T_{in} is the water temperature at the entrance of the circuit and T_{out} is the temperature at the exit. The water mass flow was obtained from the product of the flow velocity v with its density ρ and the coil's cross-sectional area A_t, seen by Equation (4). The cross-sectional area is defined as a function of the coil diameter d_S, as shown in Equation (5).

$$Q_C = n * Q_S, \tag{2}$$

$$Q_S = m_a \, c \, (T_{out} - T_{in}), \tag{3}$$

$$m_a = \rho \, A_t \, v, \tag{4}$$

$$A_t = \pi \, d_S^2 \, /4. \tag{5}$$

The problem has two unknowns, the number of circuits and the coil diameter. Hence, the heat transfer of each coil was calculated based on Newton's Cooling Law presented in Equation (6), where h is the heat transfer coefficient, A is the surface area, T_f is the water temperature and T_w is the temperature of coil's surface, as follows:

$$Q_s = h \, A \, (T_f - T_w). \tag{6}$$

Lienhard (2017) demonstrates that it's possible to determine the value of the coefficient h from the dimensionless Nusselt number, as shown in Equation (7). The Nusselt number can be described as a function of two other dimensionless numbers, seen in Equation (8), where Re_d is the Reynolds number and Pr is the Prandtl number. These are calculated from Equations (9) and (10), respectively, where μ is the fluid viscosity and k is the fluid thermal conductivity.

$$Nu_d = h\, d / k, \tag{7}$$

$$Nu_d = 0.023\, Re_d^{4/5}\, Pr^{0,4}, \tag{8}$$

$$Re_d = \rho\, d_s\, v / \mu, \tag{9}$$

$$Pr = c\, \mu / k. \tag{10}$$

From Equations (3) and (6) it was possible to determine the internal diameter of the coil of approximately 0.010 m. Thus, at least 9 circuits would be needed. After consulting a supplier's catalog, it was determined a coil diameter equals 0.00952 m (3/8") and 10 circuits. As the radiation depends on the distance between the source and the heated body, the distribution of the coils along the external surface of the chamber was proportional to the intensity of the radiation in that region. Figure 3 presents the distribution scheme in a side view of the chamber. The ends of the chamber are rounded for easy attachment of the cooling assembly to them.

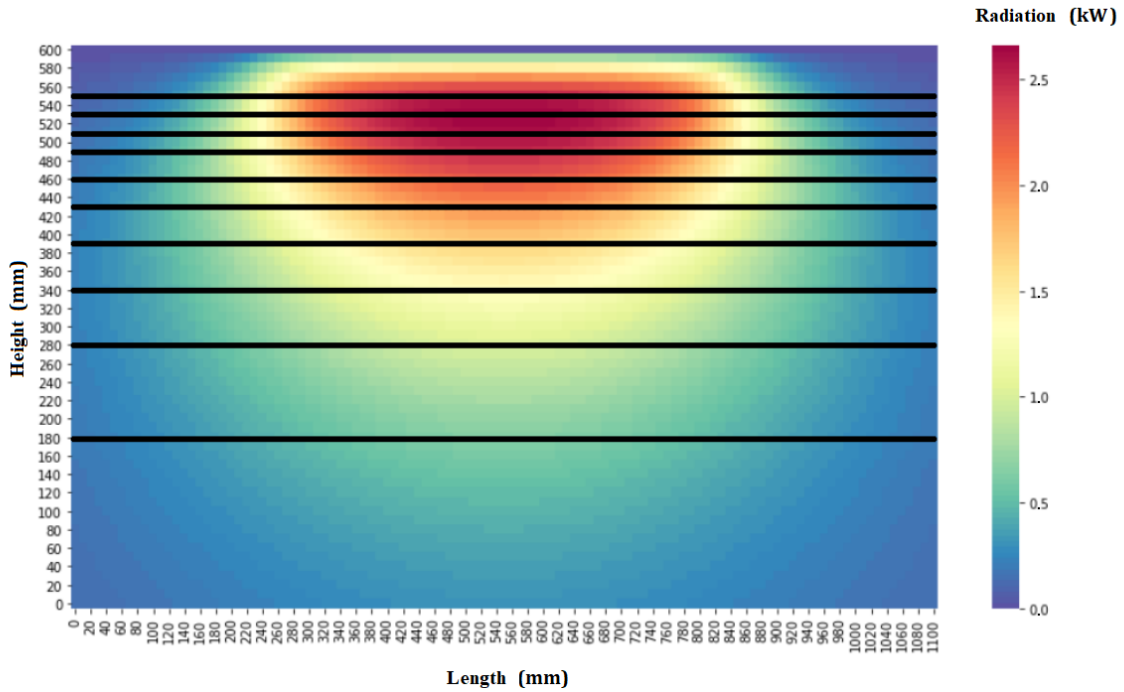

Figure 3. Serpentine distribution by radiation incident on the chamber.

It was observed that the air inside the chamber would be heated throughout the experiments and, therefore, heat transfer would occur by convection from air to the specimen. Hence, air flow is imposed at low velocity to mimic natural convection and to avoid air heating around the specimen. Air from a high pressure line in the laboratory is injected by a perforated cylinder, and then a screen-type flow conditioner is used to make the flow uniform and to avoid the appearance of temperature gradients, as shown in Figure 1. The air flow is adjusted by a needle valve.

Dhiman *et al.* (2008) presents the Richardson number Ri, which evaluates the predominance between forced and natural convection in a given flow. Equation (11) shows the definition of this dimensionless number, being a function of the Reynolds number and the Grashof number Gr, given by Equation (12). Natural convection will be predominant for Richardson number higher than 1.

$$Ri = Gr_D / Re_D^2. \tag{11}$$

$$Gr_D = g\,\beta\,(T_S - T_{inf})\,D^3 / (\mu / \rho)^2\,, \tag{12}$$

where g is the gravity acceleration, β is the thermal expansion coefficient, T_S is the surface temperature, T_{inf} is the fluid temperature and D is the outer diameter of the specimen.

The specimen diameter was defined as 0.1524 m (6 inches), maximum surface temperature of 200ºC, ambient temperature of 30ºC and a Ri value equal to 100. For natural convection to be predominant, the flow velocity must be less than or equal to 0.021 m /s.

According to Pavan (2009), the pressure loss located in the flow rectification is given by Equation (13), where K is the equipment's characteristic pressure loss coefficient and U is the flow velocity away from the specimen. The coefficient K can be estimated for low speeds by Equation (14), where a is the fraction of free area and d_m is the diameter of the mesh wire.

$$\Delta P = K\,\rho\,U^2/2, \tag{13}$$

$$K = 6.5\,(1 - a) / a^2\,(\rho\,d_m\,U / (a\,\mu))^{-1/3}. \tag{14}$$

The non-uniformity of the flow distribution in the injector is measured from the MD maldistribution parameter, defined by Senegal (1957). This parameter is calculated by Equation (15), where ΔP_o is the pressure drop in the injector orifice and ΔP_i is the pressure drop along the injector tube, defined by Equations (16) and (17), respectively.

$$MD = 1 - \sqrt{((\Delta P_o - \Delta P_i)/\Delta P_o)}. \tag{15}$$

$$\Delta P_o = 1/C_o^2\,(\rho\,U_o^2)/2, \tag{16}$$

where C_o is the orifice coefficient and U_o is the velocity of air passing through the orifice.

$$\Delta P_i = ((4\,f\,L_i) /(3\,d_i) + 1)\,(\rho\,U_i^2)/2, \tag{17}$$

where L_i is the injector tube length, d_i is the internal diameter, U_i is the inlet air velocity and f is the friction factor, defined by Equation (18).

$$f = 0.3164 / (\rho\,d_i\,U_i / \mu)^{-0.25}. \tag{18}$$

Green and Perry (2008) recommends that the MD parameter has to be less than 0.05 so the flow is satisfactorily uniform. Substituting this value in Equation (15), the relation between pressure losses along the injector and in its orifices is obtained. Thus, the relationship between internal diameter and orifice diameter is obtained as a function of the number of orifices N in the injector, described by Equation (19). An injector tube internal diameter of 0.00254 m was defined, with 10 holes, and each hole with a diameter less than 0.00313 m.

$$d_o/d_i \leq \{[(4\,L_i / (3\,d_i))\,(0.3164 / (\rho\,d_i\,U_i / \mu)^{-0.25}) + 1]\,(C_o^2\,N^2) / (1 - 0.95^2)\}^{-1/4}. \tag{19}$$

The specimen is positioned on a V-shaped support fixed in the center of the horizontal plane inside the chamber, 0.6 m under the heaters. This geometry allows evaluation of various diameters and thicknesses of shielding. A screw system adjusts the support height and inclination. A heat flux sensor and thermocouples will be installed next to the specimen. Cylindrical segments with diameters equal to 0.15 and 0.2 m (6 and 8 inches) and length up to 0.5 m will be analyzed as specimens.

3. EXPERIMENTAL PROCEDURE

The experimental procedures are organized in two phases, the first one tests the equipment and the second one performs the real measurements. The test routine of the second phase evaluates the temperature profile and heat flux along the specimen, shielded and unshielded, by imposing a controlled heat flux on it.

The distance between the specimen and the heaters is 0.1 to 0.6 m, increasing 0.1 m with each measurement. The support's inclination is from 0 to 45º, increasing 0.5º with each measurement. The range of imposed heat flux is from 5 to 10 kW/m² in the specimen. The thermal shields are made of steel plate attached to the specimen and a highly reflective paint coating (as heat insulation white paint, which shows high reflectance in the infrared spectrum).

Due to the COVID-19 pandemic, there was a delay in the delivery of the material and, consequently, the unavailability of the results of this study until the date of submission of this document.

4. References

Cavalcanti, Marcos Alexandre de Vasconcelos. Análise da influência de superfícies refletivas nas perdas de calor de sistemas térmicos. MS thesis. Universidade Federal do Rio Grande do Norte, 2011.

Dhiman, A. K., R. P. Chhabra, and V. Eswaran. "Steady mixed convection across a confined square cylinder." International communications in heat and mass transfer 35.1 (2008): 47-55.

Dornelles, Kelen Almeida, Rosana Maria Caram, and Eduvaldo Paulo Sichieri. "Absortância solar e desempenho térmico de tintas frias para uso no envelope construtivo." *http://periodicos. unb. br/index. php/paranoa* 12 (2014): 55-64.

Green, Robert H. Perry Donald W., Robert H. Perry, and Don W. Green. Perry's chemical engineers' handbook. Vol. 8. McGraw-Hill Professional Pub, 2008.

HSE. "Methods of approximation and determination of hu-man vulnerability for offshore major accident hazard as-sessment", SPC/Tech/OSD/30. London: Health and SafetyExecutive. 2006.

Kim, Sang Jin, et al. "Experimental study of the reduction of high temperatures and radiation using heat shields associated with flare towers of offshore oil and gas platforms." Ships and Offshore Structures 9.5 (2014): 540-549.

Lienhard, IV., and H. John. A heat transfer textbook. Phlogiston Press, 2017.

Muratova, E. N., et al. "Thermal radiation shielding by nanoporous membranes based on anodic alumina." Journal of Physics: Conference Series. Vol. 872. No. 1. IOP Publishing, 2017.

Ozturk, Abdurrahman. "Implementation of View Factor Model and Radiative Heat Transfer Model in MOOSE." (2019).

Pavan, L. Carlos. "Análise da distribuição de velocidade e pressão nos dutos de ar condicionado de uma aeronave regional". (2009)

Pereira, J. P. "Desenvolvimento de um compósito cerâmico para otimizar a radiação térmica em materiais refratários - Al203-SiO2-Cr203-SiC-Ca(AlO2)2." 2016.

Schwartz, R. E., and J. W. White. "Flare radiation prediction: A critical review." Paper 12a), presented at the 30th Annual Loss Prevention Symposium, American Institute of Chemical Engineers, Spring National Meeting, New Orleans, LA (Feb. 29, 1996). 0. Vol. 20. 1996.

Senegal. *Ind. Eng. Chem*., New York: McGraw-Hill, 1957,49, pp 993-997.

Viskanta, Raymond. "Effectiveness of a layer of an absorbing-scattering gas in shielding a surface from incident thermal radiation." Journal of the Franklin Institute 280.6 (1965): 483-492.

5. Responsibility notice

The authors are the only responsible for the printed material included in this paper.